Syncephalastrum massiliense sp. nov. and Syncephalastrum timoneanum sp. nov., Isolated from Clinical Samples

Jihane Kabtani , Fatima BOULANOUAR , Papa Mouhamadou GAYE , Muriel Militiello , Stéphane Ranque *

Posted Date: 11 October 2023

doi: 10.20944/preprints202310.0636.v1

Keywords: Mucormycosis; Mucorales; Syncephalastrum; genotype; phenotype

Article

Syncephalastrum massiliense sp. nov. and *Syncephalastrum timoneanum* sp. nov., Isolated from Clinical Samples

Kabtani J. [1], Boulanouar F. [1], Gaye P. M. [1], Militello M. [1,2] and Ranque S. [1,3]

[1] IHU Méditerranée Infection, 13005 Marseille, France; kabtanijihane@hotmail.com (J.K.);
[2] Aix-Marseille Université, AP-HM, IRD, SSA, MEPHI, 13005 Marseille, France
[3] Aix-Marseille Université, AP-HM, IRD, SSA, VITROME, 13005 Marseille, France
* Correspondence: to stephane.ranque@univ-amu.fr.

Abstract: Mucormycosis is known to be a rare opportunistic infection caused by fungal organisms belonging to *Mucorales* order, among them *Syncephalastrum* species. These moulds are rarely involved in clinical diseases and are generally seen as contaminants in the clinical laboratory. However, in recent years, case reports of human infections due to *Syncephalastrum* have increased, especially in immunocompromised hosts. In this study, we describe two new *Syncephalastrum* species, which were isolated from human nails and sputum samples from two different patients. We used several methods of genomic and phenotypic characterisation. The phenotypic analysis, relied on morphological features, analysed both by optical and scanning electron microscopy. We used Matrix Assisted Laser Desorption Ionization-Time of Flight mass spectrometry, energy-dispersive X-ray spectroscopy, and BiologTM technology to characterise the proteomic, chemical mapping, and carbon source assimilation profiles, respectively. The genomic analysis relied on multilocus sequence analysis of the rRNA internal transcribed spacers and D1/D2 large-subunit domains, and fragments of the translation elongation factor 1-alpha, and the β-tubulin genes. The two novel species in the genus *Syncephalastrum*, namely *S. massiliense* PMMF0073 and *S. timoneanum* PMMF0107, have a similar morphology to *S. racemosum*, but each display distinct phenotypic and genotypic features. The polyphasic approach, combining the results of complementary phenotypic and genomic assays, was instrumental in describing and characterising these two new *Syncephalastrum* species.

Keywords: mucormycosis; *Mucorales*; *Syncephalastrum*; genotype; phenotype; one new taxon

Introduction

Syncephalastrum species belong to the *Mucorales* order [1]. These species are mostly found in the environment, in tropical and subtropical areas in both the air and soil [2–4]. These are generally seen as clinical contaminants, with low pathogenicity and are rarely known to cause human diseases [5,6]. However, in recent years, case reports of human infections due to *Syncephalastrum* genus have increased significantly, especially in immunocompromised hosts with diabetes [7,8], chronic hepatorenal disease [9], corneal infections, or who have been the recipients of organ transplantations [4,10]. These human infections are usually related to the skin, nails, lungs, and central nervous system [11], and can have fatal outcomes, resulting in a highly invasive diseases [12,13]. They can also cause chronic and acute infections in immunocompetent hosts [14,15].

Mucormycosis, which is a rare opportunistic infection caused by mucorales fungi (*Lichtheimia* (40%), *Rhizopus* (30%), *Syncephalastrum* (20%) and *Rhizomucor* (10%)) [16], has become the third most common and fatal fungal infection after candidiasis and aspergillosis [10,17]. The most common species in the *Syncephalastrum* genus is *S. racemosum* [18–20]. The first report of a human infection caused by *Syncephalastrum* sp. was a cutaneous infection in an immunocompromised patient in India [20]. According to the Index Fungorum (www.indexfungorum.org), the *Syncephalastrum* genus is composed of two species: *S. racemosum* and *S. monosporum* (composed of three varieties, *S.*

 doi:10.20944/preprints202310.0636.v1

monosporum var. *monosporum*, *cristatum* and *pluriproliferum*). Recently, a third species, *S. contaminatum* was described [21].

An accurate species morphological differentiation is considerably difficult by usual mycological techniques in clinical laboratories. Different *Mucorales* genera, such as *Rhizomucor*, *Lichtheimia* and *Mucor* spp, have a laborious phenotypic identification and characterisation due to their similar morphology. Moreover, correct identification can only be achieved based on specific fungal structures. For example, *Rhizopus* spp. identification depends on the presence of rhizoids, while the lack of rhizoids is the only way to distinguish *Mucor* spp. from other *Mucorales* fungi. In practice, however, adequate fungal identification based on morphological criteria is hampered by a number of exceptions. Among the *Mucorales*, the *Cunninghamella* and *Syncephalastrum* genera can be easily recognized. *Syncephalastraceae* fungi are typified by the production of cylindrical merosporangia on the surface of fertile vesicles [22].

The high inter- and intra-species phylogenetic diversity of the *Mucorales* [15,23], is a real challenge for species identification and taxon delimitation. Numerous studies based on antifungal susceptibility tests and, more recently, on the use of molecular taxonomic methods, in particular sequencing of the Internal Transcript Spaces (ITS) 1 and 2 and the D1/D2 domains of the large subunit (LSU) of the rRNA gene, displayed more efficiency for the identification of *Mucorales* fungi than morphology-based identification [22,24]. The reliable identification of these rare infection agents is the key to further strengthening our understanding of species associated with epidemiology, pathogenicity, and outcome. This study aimed to analyse the phylogenetic status and describe the phenotypic characteristics of two new species of *Syncephalastrum* genus, relying on multilocus sequence analysis and chemical and physiological characterisation.

Methods

Fungal strains

Two novel *Syncephalastrum* strains were isolated from clinical samples from distinct patients at the University Hospital Mycology laboratory in Marseille, France. *Syncephalastrum massiliense* PMMF0073 was isolated from a sputum sample from a 53-year-old patient diagnosed with HIV in 1988 and with syphilis in 2015. This patient had recently fractured and dislocated his elbow and had a radial head prosthesis. He had suffered from headaches, intermittent fever, and generalized rashes with scratching lesions for a few months. *Syncephalastrum timoneanum* PMMF0107 was isolated from the nails of a 38-year-old patient with a history of bronchiectasis, with no exacerbation of the disease.

MALDI-TOF MS identification

The strains were inoculated on Petri dishes with Sabouraud Dextrose Agar (SDA) supplemented with Gentamycin and Chloramphenicol (GC) at 25°C between four to seven days. After growth, we proceeded to identification using Matrix-assisted Laser Desorption/ Ionization Time of Flight Mass Spectrometry (MALDI-TOF MS), following the protein extraction protocol described by Cassagne et al. (2016) [25]. The Microflex LT™ instrument and the MALDI Biotyper™ system (Bruker Daltonics GmbH, Bremen, Germany), and both the manufacturers' databases as well as an in house reference spectra database were used, as described in Normand et al. (2017) [26]. Moreover, MALDI-TOF MS spectra of the two isolates were collected, in addition to other spectra of reference strains from DSMZ and CBS collections; *S. racemosum* DSM 859, *S. monosporum* Var. *monosporum* CBS 567.91, *S. monosporum* Var. *cristatum* CBS 568.91 and *S. monosporum* Var. *pluriproliferum* CBS 569.91. All the spectra were used to construct a dendrogram based on protein expression intensity with the MALDI-TOF Biotyper Compass Explorer (Bruker Daltonics).

DNA extraction

DNA extraction was performed with the Qiagen™ Tissue kit on the EZ1 Advanced XL instrument. After five days of incubation at 25 °C on Sabouraud Dextrose agar + Gentamicin and Chloramphenicol (SDA GC), few colonies were picked from each sample, and poured into bead tubes

Preprints (www.preprints.org) | NOT PEER-REVIEWED | Posted: 11 October 2023 doi:10.20944/preprints202310.0636.v1

held in 600 µl of lysis buffer G2 (provided with the Qiagen™ Tissue kit). The next step was mechanical lysis with the FastPrep™-24 Instrument; one run at 6m/second for 40 seconds, followed by a centrifugation at 10,000 rpm for one minute. Then, 200 µl of the supernatant was poured into a flat tube provided with the kit. The extraction finally began within the EZ1 Advanced XL instrument according to the manufacturer's instructions. The total elution volume of 100 µl of genomic DNA extracted was stored at -20 °C for further analysis.

DNA amplification and sequencing

Four genes were targeted, the Internal Transcribed Spacers 1 and 2 (ITS1/ITS2) in the rRNA small-subunit (SSU), a fragment of the β-tubulin gene (TUB2), a fragment of the Translation Elongation Factor 1-alpha gene (TEF-1-α), and the D1/D2 domains of the rRNA large-subunit (LSU) (Table 1).

Table 1. Panel of primers used for amplifying ITS, TUB2, TEF-1 alpha, and D1/D2 genetic regions.

Primers	Sequences	Targeted regions	References
ITS1	TCCGTAGGTGAACCTGCGG	18S-5.8S	[27]
ITS2	GCTGCGTTCTTCATCGATGC	18S-5.8S	[27]
ITS3	GCATCGATGAAGAACGCAGC	5.8S-28S	[27]
ITS4	TCCTCCGCTTATTGATATGC	5.8S-28S	[27]
ITS1	TCCGTAGGTGAACCTGCGG	18S-5.8S, 5.8S-28S	[27]
ITS4	TCCTCCGCTTATTGATATGC	18S-5.8S, 5.8S-28S	[27]
Bt-2a	GGTAACCAAATCGGTGCTGCTTTC	TUB2	[28]
Bt-2b	ACCCTCAGTGTAGTGACCCTTGGC	TUB2	[28]
EF1-728F	CATCGAGAAGTTCGAGAAGG	TEF1	[29]
EF1-986R	TACTTGAAGGAACCCTTACC	TEF1	[29]
D1	AACTTAAGCATATCAATAAGCGGAGGA	28S	[30]
D2	GGT CCG TGT TTC AAG ACG G	28S	[30]

For each gene, the PCR Mix was prepared as followed: 5 µl of DNA extract was added to 20 µl of Mix (12.5 µl ATG (Ampli Taq Gold™ 360 Master Mix, Applied Biosystems™)/ 6 µl sterile water DNase/RNase free/ 0.75 µl Forward/Reverse primer) for achieving to a total volume of 25 µl per well. Particularly for the ITS gene, in order to ensure the entire sequence length, three PCR mixes were prepared for each sample with the ITS1/2, ITS3/4, and ITS1/4 amplifying the ITS1, ITS2, and ITS1-5.8S-ITS2 regions, respectively. The PCR programme for all fungal gene amplifications was constituted by an initial denaturation step at 95 °C for 15 minutes, followed by 39 cycles of 95 °C for one minute denaturation, 56 °C for 30 seconds annealing, 72 °C for one minute extension step, and a final extension at 72 °C for five minutes. PCR amplicons were revealed on a 2% agarose gel with the addition of Sybr SafeTM DNA gel stain (Invitrogen). The gel was visualised using the Safe Imager 2.0 Blue-Light Transilluminator™ (Invitrogen). 4 µl of the purified DNA was added to the BigDye™ mix (terminator cycle sequencing kit (Applied Biosystems)), (1 µl BD/ 1.5 µl TP/ 3 µl sterile water DNase/RNase free/ 0.5 µl Forward/Reverse primer) for achieving to a total volume of 10 µl per well. The sequencing reactions for all genomic regions, consisting of 96 °C for one minute, followed by 25 cycles of 96 °C for 10 seconds, 50 °C for five seconds, 60 °C for three minutes, were processed on a 3500 Genetic Analyzer™ (Applied Biosystems, Inc.). The sequences obtained were assembled and corrected using ChromasPro 2.0. All sequences were deposited in GenBank and the accession numbers are presented in Table 2.

Table 2. Fungal collection strain ID and GenBank accession numbers of the nucleotide sequences used in the phylogenetic analysis.

Species	Strain ID	GenBank accession numbers			
		ITS	TUB2	D1/D2	TEF1

Preprints (www.preprints.org) | NOT PEER-REVIEWED | Posted: 11 October 2023 doi:10.20944/preprints202310.0636.v1

Syncephalastrum massiliense	PMMF0073	OL699905.1	ON149883	OM417069.1	OM362516.1
Syncephalastrum timoneanum	PMMF0107	OL699906.1	ON149884	OM417070.1	OM362517.1
Syncephalastrum racemosum	DSM 859	OL699907.1	ON149885	OM417071.1	OM362518.1
S. monosporum var. monosporum	CBS 567.91	OL699908.1	ON149886	OM417072.1	OM362519.1
S. monosporum var. cristatum	CBS 568.91	OL699909.1	ON149887	OM417073.1	OM362520.1
S. monosporum var. pluriproliferum	CBS 569.91	OL699910.1	ON149888	OM417074.1	OM362521.1
Syncephalastrum racemosum	CBS 441.59	HM999985.1	NA*	MH869451.1	NA
Syncephalastrum racemosum	CBS 302.65	HM999984.1	NA	MH870214.1	NA
Syncephalastrum racemosum	CBS 213.78	HM999978.1	NA	MH872886.1	NA
Syncephalastrum racemosum	CBS 421.63	HM999973.1	NA	MH869932.1	NA
Syncephalastrum racemosum	CBS 199.81	HM999972.1	NA	HM849718.1	NA
Syncephalastrum monosporum	CBS 122.12	HM999977.1	NA	JN206575.1	NA
Syncephalastrum racemosum	EML-BT5-1	KY047152.1	NA	KY047158.1	NA
Syncephalastrum racemosum	EML-BT5-2	KY047143.1	NA	KY047157.1	NA
Microsporum canis	CBS 496.86	MH861991.1	NA	NG_069297.1	NA

*NA, not available.

Phylogenetic analysis

In addition to the sequences of the six strains, we added eight other reference strain sequences obtained from the GenBank database (Accession numbers are presented in Table 2). Two phylogenetic trees were constructed using the Maximum Parsimony (MP) method, with the MEGA (Molecular Evolutionary Genetics Analysis) software version 11 [31] by using the default settings, and 1,000 bootstrap replications to assess branch robustness. The first tree was based on the concatenated ITS and D1/D2 sequences of all the strains. The second tree was only based on the concatenated ITS, TUB2, TEF-1-α, and D1/D2 sequences of the six following strains: *Syncephalastrum massiliense* PMMF0073, *Syncephalastrum timoneanum* PMMF0107, *S. racemosum* DSM 859, *S. monosporum var. monosporum* CBS 567.91, *S. monosporum var. cristatum* CBS 568.91 and *S. monosporum var. pluriproliferum* CBS 569.91. *Microsporum canis* CBS 496.86 was used as an outgroup. A Bayesian phylogenetic inference was also achieved. Two other multi locus phylogenetic trees were constructed with MrBayes software (3.2.7a) and Figtree (V.1.4.4).

Macroscopic characterisation

To study their growth temperature profiles and macroscopic characters such as time of growth, colony morphology, surface and reverse colours, the six strains were cultivated on SDA GC plates for seven days. They were then subcultured on other SDA GC plates, which were incubated at different temperatures: 4 °C, 25 °C, 30 °C, 37 °C, 40 °C, and 45 °C; and on a dehydrated medium (peptone: 5 g/l; glucose: 10 g/l; potassium dihydrogen phosphate: 1 g/l; magnesium sulfate: 0.5 g/l; dichloran: 0.002 g/l; chloramphenicol: 50mg/l; agar: 15g/l; pH: 5.6 ± 0.2) at 30 °C.

Microscopic characterisation

To compare the microscopic features of the different fungal structures (hyphae, spores, and vesicles), fresh cultures of the six strains on SDA GC were first of all examined by optical microscopy. Slides were prepared by gently dabbing the surface of the fungal colony with adhesive tape. The tape

 doi:10.20944/preprints202310.0636.v1

was then mounted with one drop of lactophenol cotton blue between the slide and the slip cover. Photographs were taken with DM 2500 (Leica Camera SARL, Paris, France).

Scanning Electron Microscopy (SEM) was performed with the TM4000 Plus (Hitachi High-Technologies, Tokyo, Japan) microscope using the 15KeV lens mode 4 with a Back-Scattered Electron detector. A fungal colony sample was cut from the petri dish and placed on a microscopy slide. A volume of 400 μl of 2.5% glutaraldehyde in 0.1M sodium cacodylate buffer was poured over the fungal cut for fixation and stored at 30 °C until completely dry. Standardised fungal structures (hyphae, vesicle, sporangiola, merosporangium and the number of sporangiospores within the merosporangial sack) were measured using a specific tool for distance measurement included in the TM4000 Plus microscope. The results are represented in a Principal Component Analysis (PCA) computed with the XLSTAT (Addinsoft, Paris, France) software.

Physiological analysis

1. EDX (Energy-Dispersive X-ray Spectroscopy)

Fresh colonies of the six strains were fixed for at least one hour with glutaraldehyde 2.5% in 0.1M sodium cacodylate buffer. Cytospin was performed using a volume of 200 μl from the fixed solution, followed by a centrifugation at 800 rpm for eight minutes. EDX was carried out with an INCA X-Stream-2 detector (Oxford Instruments) linked to the TM4000 Plus SEM and AztecOne software (Oxford instruments). The slide chemical mapping was performed blindly, and all chemical elements were taken into account. Weight and atomic percentages were subjected to a PCA computed with the XLSTAT (Addinsoft) software.

2. Biolog™ phenotypic analysis

The phenotypic analysis was achieved using Biolog™ advanced phenotypic technology as previously used for yeasts characterisation by Kabtani et al. (2022) [32]. This system aims to characterise microorganisms by using a patented Redox tetrazolium dye that changes colour in response to cellular respiration in 96 micro well plates that confers a metabolic fingerprint. We used the FF (Filamentous Fungi) MicroPlates (Gen III), for carbon sources utilisation. The carbon sources were selected for their high discrimination between fungal phenotype profiles [33]. All wells contained the substrate and the dye, with the exception of the control well that only contained the dye. The strains were first cultivated on Malt Extract Agar (MEA) 2% medium, prepared with 20 g/l malt extract and 18 g/l agar in distilled water [34]. The fungal incubation time depended on its specific growth rate. The *Syncephalastrum* is a fast-growing genus that reaches its maximal growth after five to seven days. After colonies had developed and the hyphae colour had turned from white to dark brown, the fungal suspension was prepared in the FF inoculating fluid (Biolog part number 72106) by swabbing the surface of the colony. Transmittance levels were adjusted between 75% and 80% using a Biolog™ Turbidimeter [33]. The assay was performed in triplicate, 100 µl of the suspension were poured into each well of the FF MicroPlates (Biolog part number 1006), that were incubated at 26 °C for seven days, and read using the Biolog MicroStation™ Reader. The results were represented as a heat map, performed using the XLSTAT™ (Addinsoft) software.

Antifungal Susceptibility Testing (AFST)

We determined the in vitro activity of ten antifungal drugs, namely amphotericin B, voriconazole, posaconazole, itraconazole, isavuconazole, fluconazole, micafungin, anidulafungin, flucytosine, and caspofungin, against the two clinical isolates and the four type strains of *Syncephalastrum* genus. The minimal inhibitory concentration of each antifungal was determined using E-test™ (bioMérieux, Craponne, France) concentration gradient agar diffusion assay, as described in Kondori et al. (2011) [34].

Results

Preprints (www.preprints.org) | NOT PEER-REVIEWED | Posted: 11 October 2023 doi:10.20944/preprints202310.0636.v1

MALDI-TOF MS identification

The MALDI-TOF MS identification of the new isolates, *Syncephalastrum massiliense* PMMF0073 and *Syncephalastrum timoneanum* PMMF0107, did not match with any spectrum present in our laboratory database. The strains spectra did, however, reveal pertinent information about protein expression profiles that was interesting for strain differentiation. The dendrogram (Figure 1) revealed the similarity of each isolate with a distinct *Syncephalastrum* species. *Syncephalastrum timoneanum* PMMF0107 clustered with *S. racemosum* DSM 859 and *Syncephalastrum massiliense* PMMF0073 clustered with the *S. monosporum* clade.

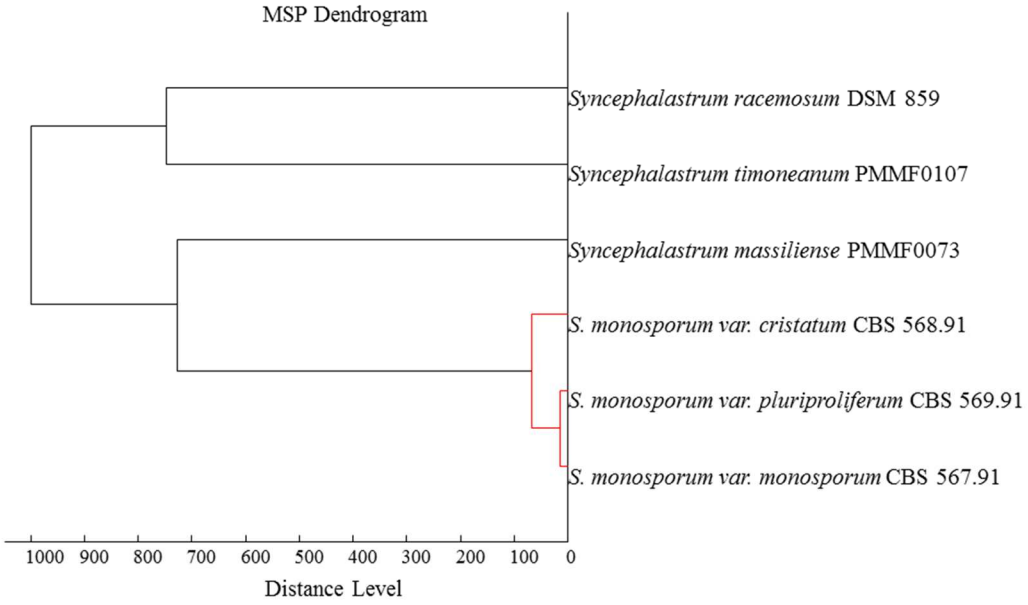

Figure 1. MALDI-TOF MS dendrogram based on protein expression intensity profile for 4 reference strains and 2 new species of *Syncephalastrum*, generated by the MALDI-TOF Biotyper Compass Explorer software (Bruker Daltonics).

DNA sequencing and phylogenetic analysis

The ITS region is recognised as the most precise and distinct marker in *Mucorales* (Ramesh et al. 2010). However, the two isolate sequences (accession numbers provided in Table 2) queried using the search tool (BLAST/NCBI) (http://blast.ncbi.nlm.nih.gov/blast) against the NCBI nucleotide database showed less than 98% identity with available nucleotide sequences, which was below the usual species identification threshold. Four dendrograms were built. The first were based on the concatenation of the ITS and D1/D2 sequences of 14 strains. The second were based on the concatenation of four loci (ITS, TEF1, TUB2 and D1/D2) of six strains. In the first trees (Figures 2 and 4), each new isolates clustered in a distinct clade. *Syncephalastrum massiliense* PMMF0073 appeared closely related to *S. racemosum*, while *Syncephalastrum timoneanum* PMMF0107 appeared relatively distant from both *S. racemosum* and *S. monosporum*. Furthermore, the second trees (Figure 3, 5) illustrated the distinct genomic features of the two novel species, which were relatively distant from one another, each clustering with a distinct *Syncephalastrum* species: *S. timoneanum* PMMF0107 with *S. racemosum*, and *S. massiliense* PMMF0073 with *S. monosporum*.

Preprints (www.preprints.org) | NOT PEER-REVIEWED | Posted: 11 October 2023 doi:10.20944/preprints202310.0636.v1

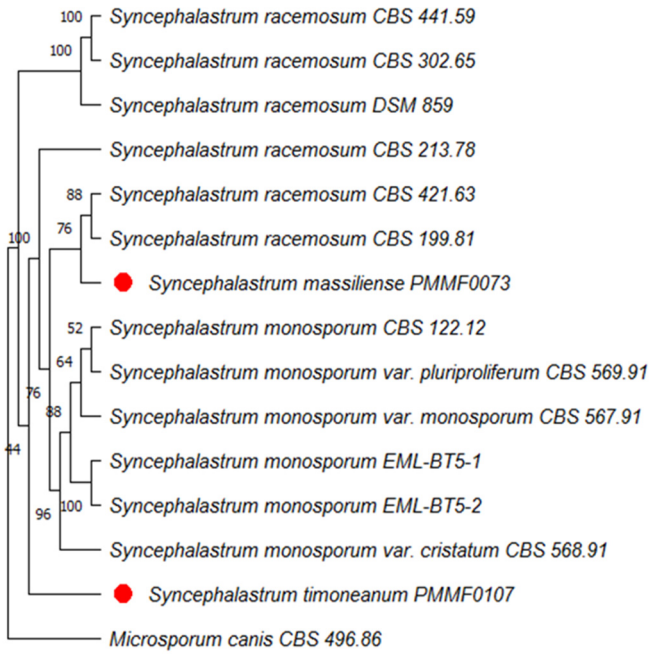

Figure 2. Maximum parsimony dendrogram based on the concatenated ITS and D1/D2 sequences, including *Syncephalastrum massiliense* PMMF0073, *Syncephalastrum timoneanum* PMMF0107, and 8 other *Syncephalastrum* spp. reference strains. *Microsporum canis* CBS 496.86 was used as outgroup. The tree was constructed with the maximum parsimony method using MEGA 11 software. Bootstrap values were estimated at 1000 replications.

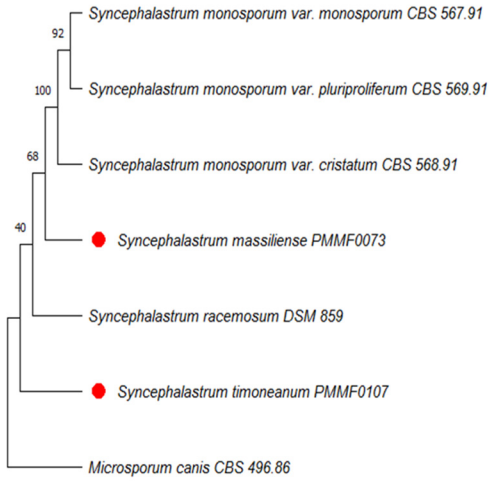

Figure 3. Maximum parsimony dendrogram based on the concatenated ITS, TUB2, TEF1 and D1/D2 sequences of *Syncephalastrum massiliense* PMMF0073, and *S. timoneanum* PMMF0107, and 4 *Syncephalastrum* spp. type strain. *Microsporum canis* CBS 496.86 was used as outgroup. The tree was constructed with the maximum parsimony method using the MEGA 11 software. Bootstrap values were estimated at 1000 replications.

Preprints (www.preprints.org) | NOT PEER-REVIEWED | Posted: 11 October 2023 doi:10.20944/preprints202310.0636.v1

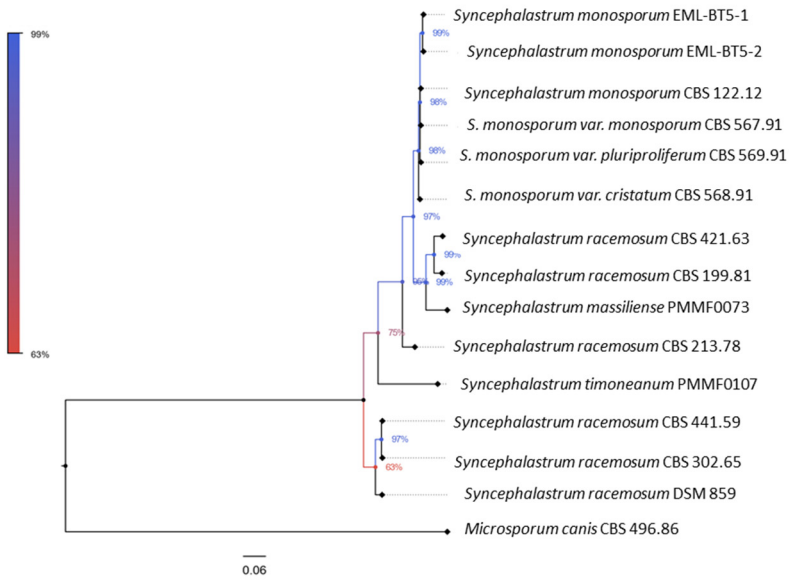

Figure 4. Bayesian phylogenetic tree based on the concatenated ITS and D1/D2 sequences of Syncephalastrum massiliense PMMF0073, and S. timoneanum PMMF0107, and 4 Syncephalastrum spp. type strain. Microsporum canis CBS 496.86 was used as outgroup. The tree was constructed with MrBayes software (3.2.7a) and Figtree (V.1.4.4).

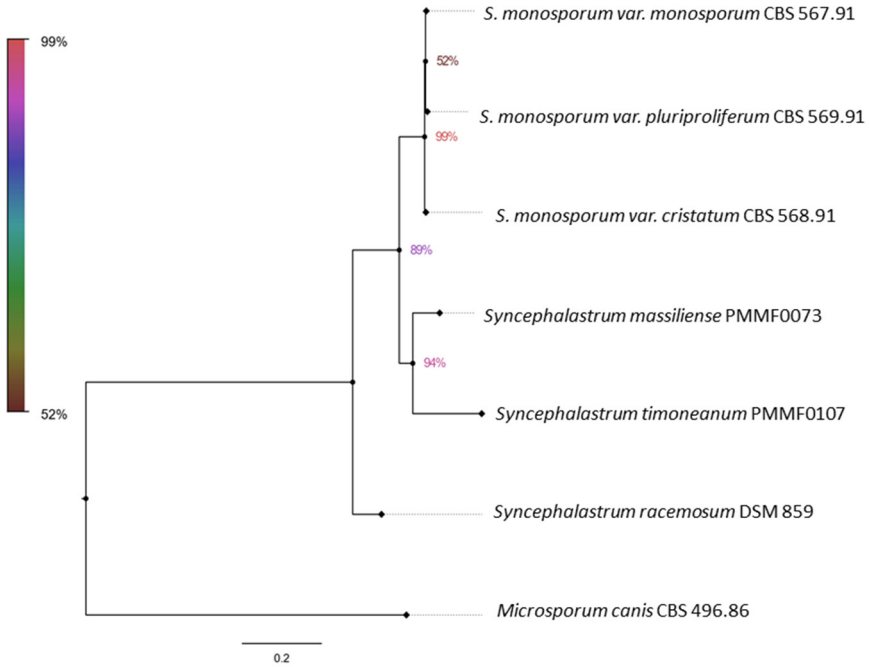

Figure 5. Bayesian phylogenetic tree based on the concatenated ITS, TUB2, TEF1 and D1/D2 sequences of Syncephalastrum massiliense PMMF0073, and S. timoneanum PMMF0107, and 4 Syncephalastrum spp. type strain. Microsporum canis CBS 496.86 was used as outgroup. The tree was constructed with MrBayes software (3.2.7a) and Figtree (V.1.4.4).

Preprints (www.preprints.org) | NOT PEER-REVIEWED | Posted: 11 October 2023 doi:10.20944/preprints202310.0636.v1

Macroscopic characterisation

The macroscopic morphological features of the six strains were a rapid time of growth on SDA GC medium, with an optimal growth temperature of 25°C. Colonies with a fluffy and cottony aspect appeared after two to three days of incubation. The colour of the Mycelium was white after 48 hours, then became darker after 72 hours, and reached a high level of sporulation around day five. The mycelium of *Syncephalastrum massiliense* PMMF0073, *Syncephalastrum timoneanum* PMMF0107, and *S. monosporum var. monosporum* CBS 567.91 was dark in colour, while it was grey for *S. monosporum var. cristatum* CBS 568.91 and *S. monosporum var. pluriproliferum* CBS 569.91. *S. racemosum* DSM 859 displayed a lighter colour. All isolates were xerotolerant, as they grew on dehydrated medium. None of them grew at 4°C, 40°C, or 45°C (Figure 6).

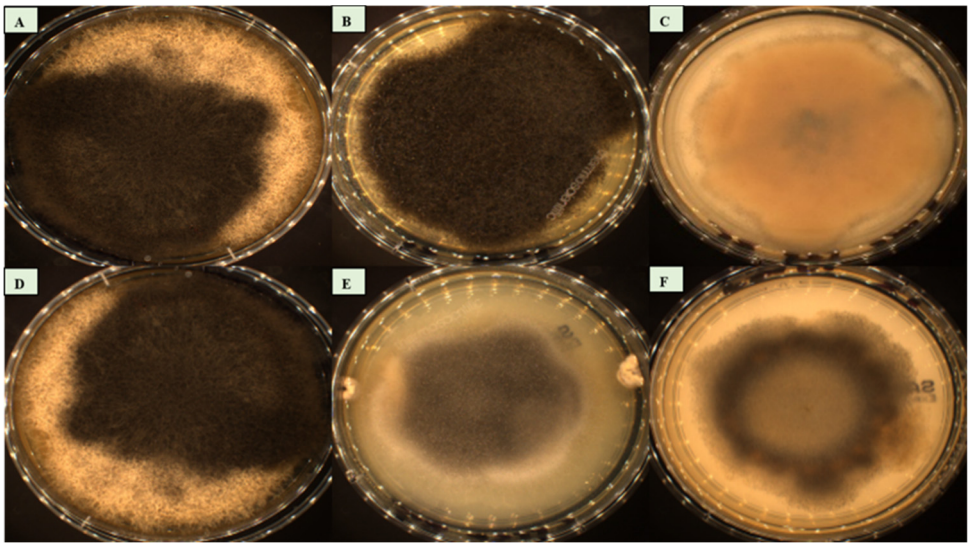

Figure 6. Culture growth on SDA GC at 25°C. **A:** Syncephalastrum massiliense PMMF0073. **B:** Syncephalastrum timoneanum PMMF0107. **C:** S. racemosum DSM 859. **D:** S. monosporum var. monosporum CBS 567.91. **E:** S. monosporum var. cristatum CBS 568.91. **F:** S. monosporum var. pluriproliferum CBS 569.91.

Microscopic characterisation

Microscopic observation revealed irregular branched wide hyphae (sporangiophores), aseptate with a ribbon-like aspect, in addition to an ovoid and globose terminal vesicle at the apices for all the strains, with different lengths. Depending on the species, the terminal vesicle generates cylindrical merosporangia over the whole surface, containing several spores in a single row.

S. monosporum species presented the largest hyphae (13-17 μm) and smallest vesicle (15-28 μm) in comparison with *Syncephalastrum massiliense* PMMF0073, *Syncephalastrum timoneanum* PMMF0107 and *S. racemosum* DSMZ 859 which, in contrast, displayed smaller hyphae (7-11 μm) and larger vesicle (29-31 μm). The surface of *S. monosporum* vesicle was entirely covered by sporangiola (4-7 μm). However, the vesicle surfaces of *Syncephalastrum massiliense* PMMF0073, *Syncephalastrum timoneanum* PMMF0107 and *S. racemosum* DSMZ 859 were all surrounded by grey cylindrical merosporangia (15-16 μm). Each merosporangial sack contained six or seven light-grey merospores, smooth-walled and spherical to ovoid (3-6 μm). Rhizoids were occasionally observed (Figures 7 and 8). A PCA based on fungal structures measures showed that the microscopic features of the two new strains were relatively similar to *S. racemosum* (Figure 9).

Preprints (www.preprints.org) | NOT PEER-REVIEWED | Posted: 11 October 2023 doi:10.20944/preprints202310.0636.v1

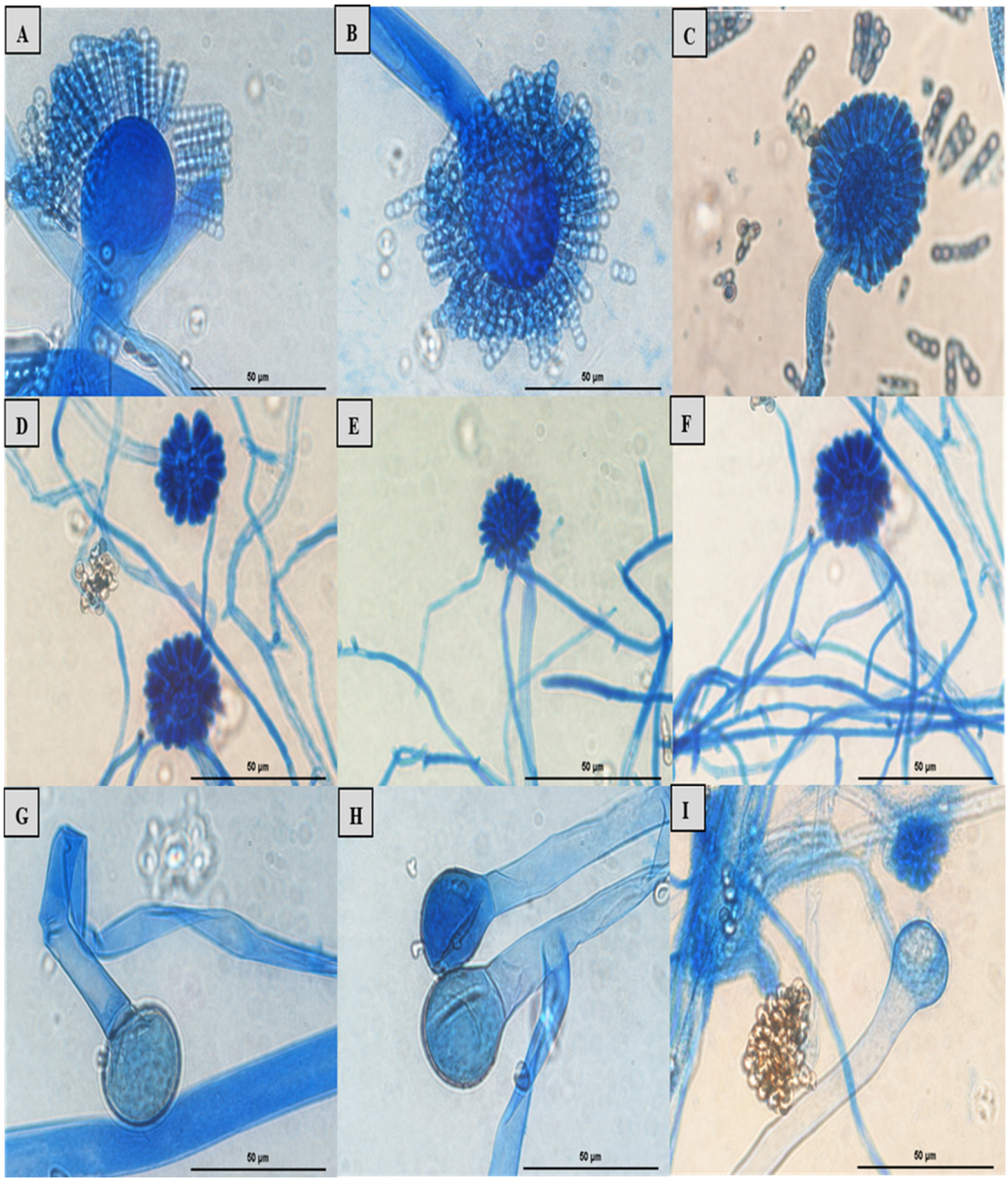

Figure 7. Lactophenol cotton blue mount of *Syncephalastrum* spp. **A, B, C:** sporangiophore with apical vesicle and merosporangial sacks enclosing merospores of *Syncephalastrum massiliense* PMMF0073, *Syncephalastrum timoneanum* PMMF0107 and *S. racemosum* DSM 859. **D, E, F:** sporangiophore with apical vesicle and sporangiola of *S. monosporum var. monosporum* CBS 567.91, *S. monosporum var. cristatum* CBS 568.91 and *S. monosporum var. pluriproliferum* CBS 569.91. **G:** columella and hyphae ribbon like aspect of *Syncephalastrum timoneanum* PMMF0107. **H, I:** columella of *S. racemosum* and *S. monosporum*. Optical microscopy (Magnification x1000). Scale bars: 50 μm.

Preprints (www.preprints.org) | NOT PEER-REVIEWED | Posted: 11 October 2023 doi:10.20944/preprints202310.0636.v1

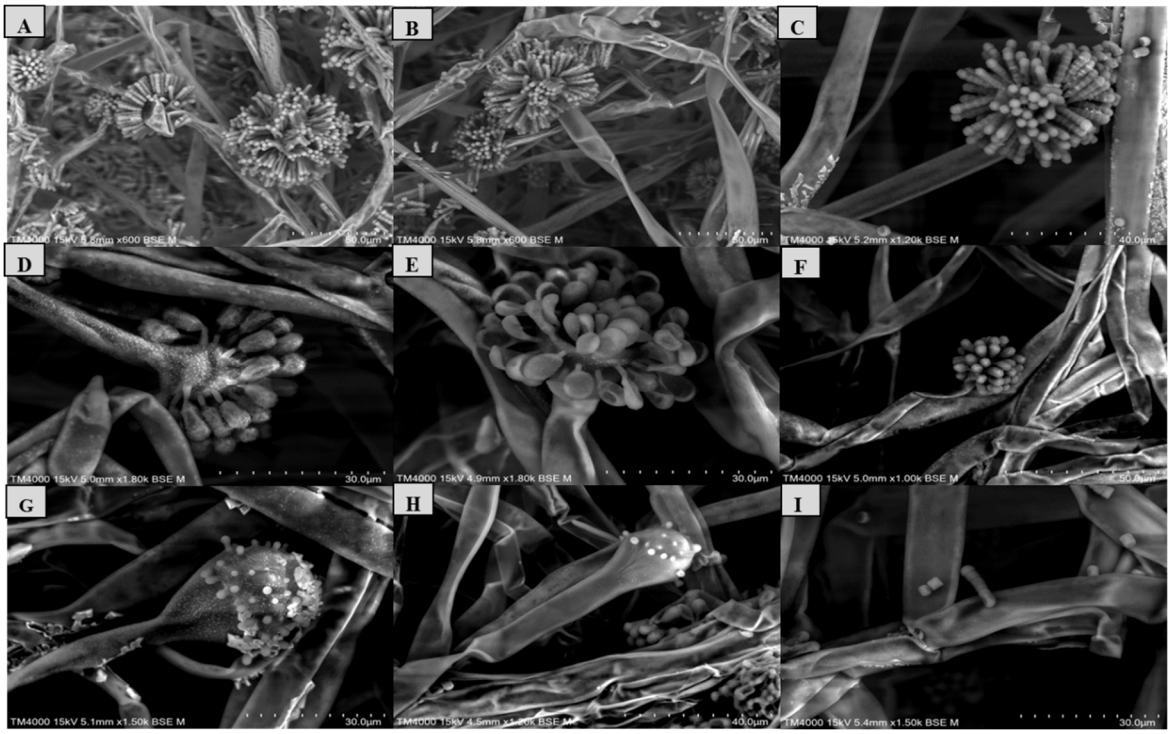

Figure 8. Morphology of *Syncephalastrum* spp. **A, B, C:** sporangiophore with apical vesicle and merosporangial sacks of *Syncephalastrum massiliense* PMMF0073, *Syncephalastrum timoneanum* PMMF0107 and *S. racemosum* DSM 859. **D, E, F:** sporangiophore with apical vesicle and sporangiola of *S. monosporum var. monosporum* CBS 567.91, *S. monosporum var. cristatum* CBS 568.91 and *S. monosporum var. pluriproliferum* CBS 569.91. **G, H:** columella of *S. racemosum* and *S. monosporum*. I: merosporangium sack with 6 merospores of *S. racemosum*. Scanning Electron Microscopy TM 4000Plus (15KeV lens mode 4). Scale bars: **A, B, F** = 50μm, **C, H** = 40 μm, **D, E, G, I** =30 μm.

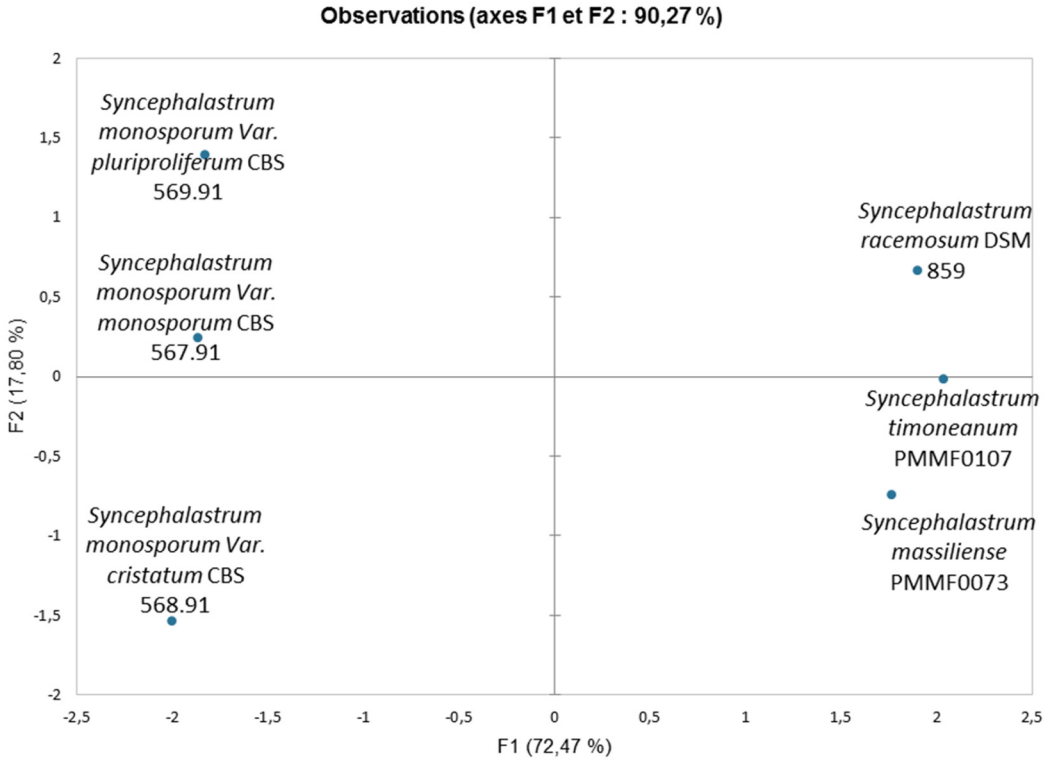

Figure 9. Principal Component Analysis (PCA) of different structures measurements (hyphae, columella, sporangiola, merosporangium and sporangiospores number within the merosporangial

Preprints (www.preprints.org) | NOT PEER-REVIEWED | Posted: 11 October 2023 doi:10.20944/preprints202310.0636.v1

sack) using TM4000 Plus microscope (SEM) for 4 reference strains and two new species of *Syncephalastrum*. In this analysis, computed with the XLSTAT software, the principal components F1 and F2 explained 90.3% of the fungi structures variance.

Physiological analysis

1. EDX (Energy-Dispersive X-ray Spectroscopy)

The results are represented as a PCA (Figure 10), showing that the chemical mapping profiles of the two new species differed from those of *S. racemosum* DSM 859. *Syncephalastrum timoneanum* PMMF0107 clustered with *S. monosporum var. monosporum* CBS 567.91, while *Syncephalastrum massiliense* PMMF0073 clustered with both *S. monosporum var. cristatum* CBS 568.91 and *S. monosporum var. pluriproliferum* CBS 569.91.

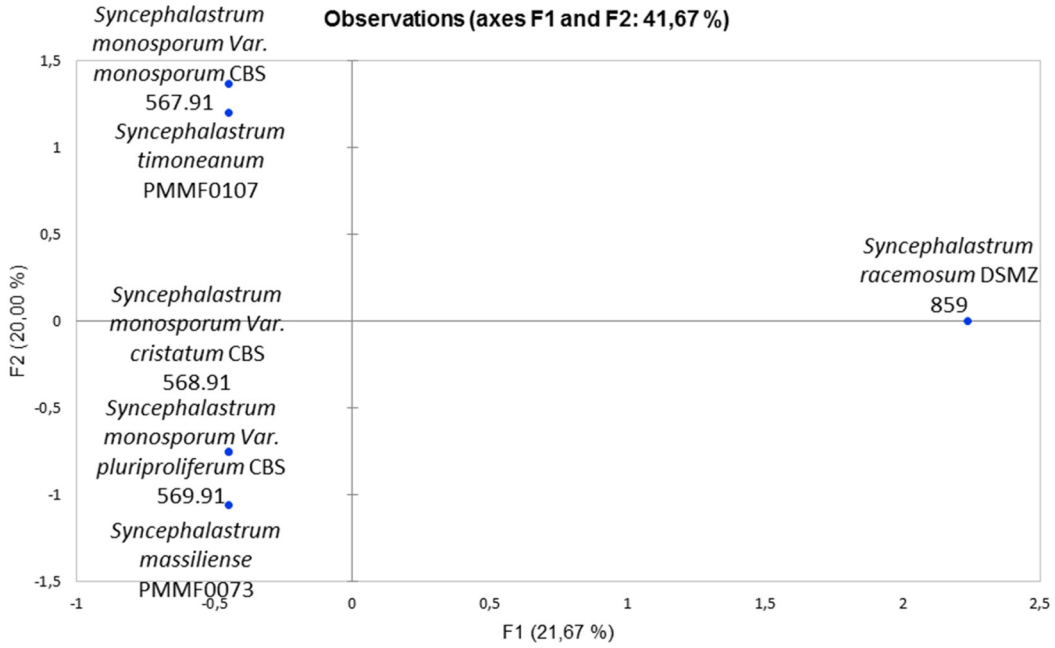

Figure 10. Principal Component Analysis of the EDX (Energy-Dispersive X-ray Spectroscopy) chemical mapping profile of 4 reference strains and the 2 novel *Syncephalastrum* species, In this analysis, computed with the XLSTAT software, the principal components F1 and F2 explained 41.7% of the EDX data variance.

2. Biolog™ system

The Biolog™ phenotypic technology provides valuable information about strain properties using a specific and precise microbial phenotypic characterisation. When reduction occurs in FF plates, the dye colour changes to purple. The Biolog Omnilog equipment analyses images taken over time with a colour camera to quantify the reduced dye (Bochner et al. 2001). The results are represented as a heat map (Figure 11), which appears fairly heterogeneous, showing that each new species has a substrate assimilation profile close to a distinct *Syncephalastrum* species. Most of the substrates were assimilated. The few non assimilated substrates were instrumental for species discrimination. *Syncephalastrum timoneanum* PMMF0107 appeared relatively close to *S. monosporum*. In contrast, *Syncephalastrum massiliense* PMMF0073 appeared closer to *S. racemosum*.

Preprints (www.preprints.org) | NOT PEER-REVIEWED | Posted: 11 October 2023 doi:10.20944/preprints202310.0636.v1

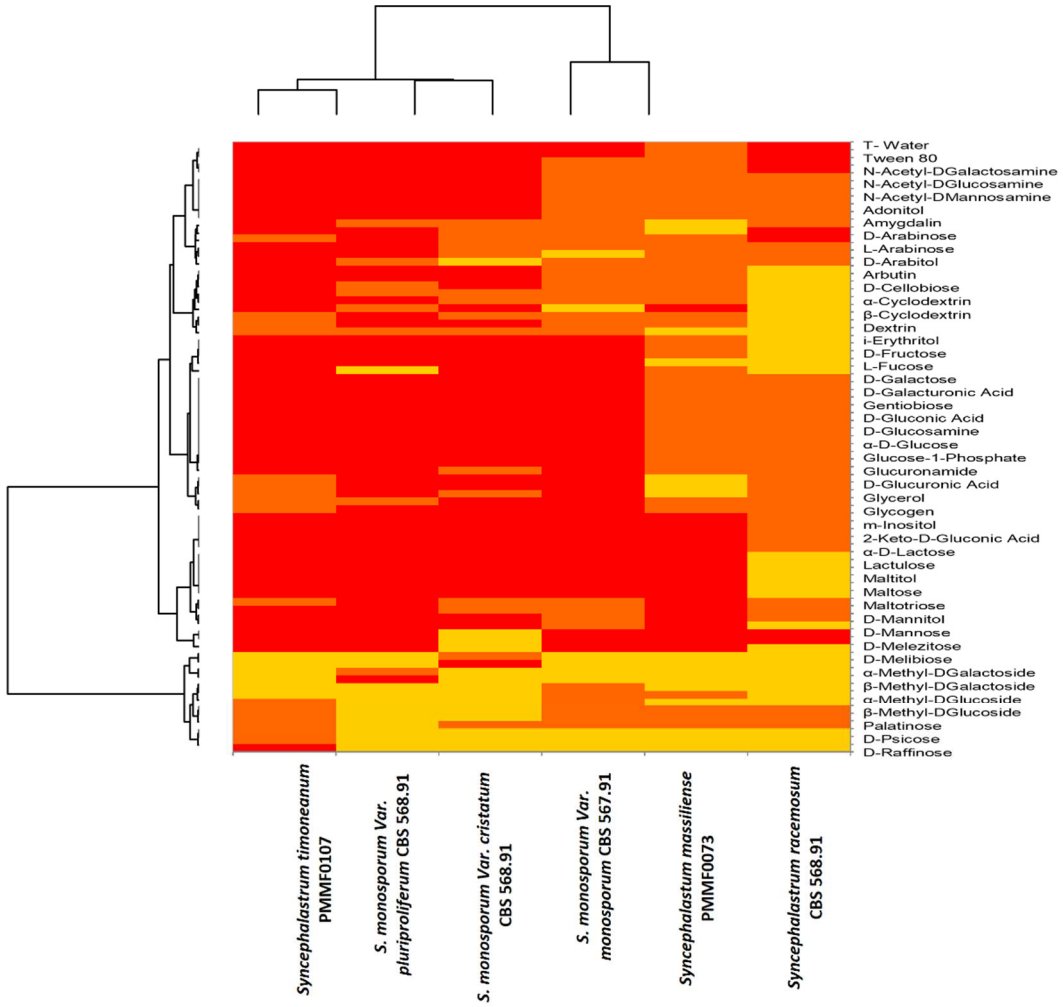

Figure 11. Heat Map of carbon sources assimilation assessed by Biolog™ system, for 4 reference strains and two species of *Syncephalastrum*, computed with the XLSTAT software. Color gradient interpretation: the most assimilated substrate are in red, and the least assimilated substrate in yellow.

Antifungal Susceptibility Testing (AFST)

The minimal inhibitory concentrations (MICs) of the ten antifungal drugs evaluated are displayed in (Table 3). All strains exhibited high micafungin, anidulafungin, caspofungin, flucytosine, fluconazole, voriconazole, and isavuconazole MICs. Amphotericin B and itraconazole MICs were relatively low against *S. massiliense* PMMF0073, *S. timoneanum* PMMF0107 and *S. racemosum* DSM 859. Whereas, posaconazole MICs were only low against *S. timoneanum* PMMF0107 and *S. racemosum* DSM 859. Noteworthy, itraconazole and posaconazole MICs were lower against *S. timoneanum* PMMF0107 and *S. racemosum* DSM 859 than against *S. massiliense* PMMF0073.

Table 3. E-test minimal inhibitory concentrations (MICs) of ten antifungal drugs against six refrence *Syncephalastrum* strains, including the two novel species: *S. massiliense*, and *S. timoneanum*.

MIC (mg/l)	AMB	AND	CAS	MIC	5-FC	FL	ITC	POS	VOR	IS*
Syncephalastrum massiliense PMMF0073	0.125	>32	>32	>32	>32	>256	4	>32	>32	>32
Syncephalastrum timoneanum PMMF0107	0.047	>32	>32	>32	>32	>256	1	6	>32	>32
Syncephalastrum racemosum DSM 859	0.25	>32	>32	>32	>32	>256	0.75	0.75	>32	>32

Preprints (www.preprints.org) | NOT PEER-REVIEWED | Posted: 11 October 2023 doi:10.20944/preprints202310.0636.v1

S. monosporum var. monosporum CBS 567.91	>32	>32	>32	>32	>32	>256	>32	>32	>32	>32
S. monosporum var. cristatum CBS 568.91	>32	>32	>32	>32	>32	>256	>32	>32	>32	>32
S. monosporum var. pluriproliferum CBS 569.91	>32	>32	>32	>32	>32	>256	>32	>32	>32	>32

*AMB, amphotericin B; * AND, anidulafungin; CAS, caspofungin; MIC, micafungin; 5-FC, flucytosin; FL, fluconazole; ITC, itraconazole; POS, Posaconazole; VOR, voriconazole; and IS isavuconazole.

Figure 8. Morphology of *Syncephalastrum* spp. **A, B, C:** sporangiophore with apical vesicle and merosporangial sacks of *Syncephalastrum massiliense* PMMF0073, *Syncephalastrum timoneanum* PMMF0107 and *S. racemosum* DSM 859. **D, E, F:** sporangiophore with apical vesicle and sporangiola of *S. monosporum* var. *monosporum* CBS 567.91, *S. monosporum* var. *cristatum* CBS 568.91 and *S. monosporum* var. *pluriproliferum* CBS 569.91. **G, H:** vesicle of *S. racemosum* and *S. monosporum*. I: merosporangium sack with 6 merospores of *S. racemosum*. Scanning Electron Microscopy TM 4000Plus (15KeV lens mode 4). Scale bars: **A, B, F** = 50μm, **C, H** = 40 μm, **D, E, G, I** =30 μm.

Taxonomy

Syncephalastrum massiliense Kabtani J. and Ranque S. sp. nov.

MycoBank: MB843858
(Fig 7-A, Fig 8-A)

Etymology: Named after Marseille, the city where it was isolated.

Diagnosis: *Syncephalastrum massiliense* PMMF0073 is closely similar to *S. racemosum* DSMZ 859, based on microscopic characters. Both species present small hyphae (7-11 μm) and large vesicle (29-31 μm), in contrast with *S. monosporum* that present larger hyphae (13-17 μm) and smaller vesicle (15-28 μm). Moreover, *S. monosporum* vesicle surface is entirely covered by sporangiola (4-7 μm). Meanwhile, both *S. massiliense* PMMF0073 and *S. racemosum* DSMZ 859 vesicle surfaces are surrounded by merosporangia (15-16 μm). Each merosporangial sack contains six or seven merospores.

Type: **France**: Marseille. Human sputum, 11 September 2019. (PMMF0073 – holotype; IHEM 28561 - isotype). GenBank: OL699905 (ITS), ON149883 (Btub2), OM362516 (TEF-1a), OM417069 (D1/D2).

Description: Macroscopic features showed that *Syncephalastrum massiliense* has a rapid growth time on SDA GC medium, with an optimal temperature of growth at 25 °C. The strain was xerotolerant, and growth was inhibited at temperatures ≤4 °C or ≥40 °C. Colonies with fluffy and cottony aspect were seen from two to three days post-inoculation. The mycelium was white at 48 hours then became darker at 72 hours and reached a high sporulation level around day five. Microscopic observation revealed wide hyphae (sporangiophores), aseptate with a ribbon-like aspect, and an ovoid globose terminal vesicle at the apices. *Syncephalastrum massiliense* presented small hyphae (7–11 μm) and larger vesicle (29–31 μm). The vesicle surface was entirely surrounded by merosporangia (15-16 μm). Each merosporangial sack contained six or seven sporangiospores (merospores). A few rhizoids were observed.

The Biolog™ phenotypic technology provided information on the assimilation capacity of the fungus carbon sources. *S. massiliense* PMMF0073 was the only *Syncephalastrum* tested that assimilated the least substrates, including adonitol, alpha-methyl-D-glucoside, trehalose, turanose, succinic acid mono-methyl ester, and alaninamide. It was noteworthy that D-tagatose was only assimilated by *S. massiliense* PMMF0073 and *S. monosporum* var. *monosporum* CBS 567.91. *S. massiliense* PMMF0073 displayed a carbon source assimilation profile relatively similar to *S. racemosum* DSM 859.

Host: Human

 doi:10.20944/preprints202310.0636.v1

Syncephalastrum timoneanum Kabtani J. and Ranque S. sp. nov.

MycoBank: MB843870

(Fig 7-B, Fig 8-B)

Etymology: Named after La Timone, the hospital where it was isolated in Marseille, France.

Diagnosis: *Syncephalastrum timoneanum* PMMF0107 is closely related to *S. racemosum* DSMZ 859, relying on microscopic characteristics. The two species present small hyphae (7-11 μm) and large vesicle (29-31 μm), in contrast to *S. monosporum* species which has larger hyphae (13-17 μm) and smaller vesicle (15-28 μm). In addition, while the vesicle surface of *S. monosporum* is fully covered by sporangiola (4-7 μm), the vesicle surface of both *S. timoneanum* PMMF0107 and *S. racemosum* DSMZ 859 was surrounded by merosporangia (15-16 μm). Each merosporangial sack contained six or seven sporangiospores (merospores).

Type: **France**: Marseille. Human nails, 02 March 2020. (PMMF0107 – holotype; IHEM 28562 - isotype). GenBank: OL699906 (ITS), ON149884 (Btub2), OM362517 (TEF-1a), OM417070 (D1/D2).

Description: Macroscopic features revealed that *Syncephalastrum timoneanum* PMMF0107 has a rapid growth time on SDA GC medium, with an optimal temperature of growth at 25 °C. The strain can grow on dehydrated medium, demonstrating that is xerotolerant. However, no growth was observed at 4 °C, 40 °C, and 45°C. Colonies with a fluffy and cottony aspect were seen from two to three days. The colour of the mycelium was white in the first 48 hours, then became darker at 72 hours and reached a high level of sporulation around day five. Microscopic observation showed wide hyphae (sporangiophores) and aseptate with a ribbon-like aspect, in addition to an ovoid and globose terminal vesicle at the apices. *Syncephalastrum timoneanum* PMMF0107 exhibited small hyphae (7–11 µm) and large vesicle (29–31 µm). The surface of its vesicle was entirely covered by merosporangia (15–16 µm). Each merosporangial sack contained about six or seven sporangiospores (merospores). Some rhizoids were observed.

The Biolog™ advanced phenotypic technology provided information on the assimilation capacity of the fungus carbon sources. *S. timoneanum* PMMF0107 was the only species of *Syncephalastrum* genus that assimilated most of substrates. However, there was some exceptional substrates that were not assimilated (D-tagatose, D-psicose, N-acetyl-D-mannosamine, L-fucose, glucuronamide, sedoheptulosan). Based on this carbon source assimilation, *S. timoneanum* PMMF0107 displays a relatively similar profile to *S. monosporum* species.

Host: Human

Additional specimen examined (1): Type: **Country of origin unknown**. Before 24 January 1977. (DSM 859 - holotype; ATCC 18192 - isotype). GenBank: OL699907 (ITS), ON149885 (Btub2), OM362518 (TEF-1a), OM417071 (D1/D2).

Additional specimen examined (2): Type: **China:** Zhejiang Prov., Wuxing. Soil, 21 October 1960. (CBS 567.91 - holotype). GenBank: OL699908 (ITS), ON149886 (Btub2), OM362519 (TEF-1a), OM417072 (D1/D2).

Additional specimen examined (3): Type: **China:** Jiangsu Prov., Nanjing. Soil, 13 October 1960. (CBS 568.91 - holotype). GenBank: OL699909 (ITS), ON149887 (Btub2), OM362520 (TEF-1a), OM417073 (D1/D2).

Additional specimen examined (4): Type: **China:** Zhejiang Prov., Hangzhou. Pit mud, 19 October 1960. (CBS 569.91 - holotype). GenBank: OL6999010 (ITS), ON149888 (Btub2), OM362521 (TEF-1a), OM417074 (D1/D2).

Discussion

In this study, we propose that *Syncephalastrum massiliense* PMMF0073, isolated from human sputum, and *Syncephalastrum timoneanum* PMMF0107, isolated from human nails, are two novel species in the *Syncephalastrum* genus based on their comprehensive phenotypic and genotypic analysis. The phenotypic analysis highlighted the distinct protein expression profiles of these two isolates assessed using MALDI-TOF MS. Each one appeared closer to a different species of the

 doi:10.20944/preprints202310.0636.v1

Syncephalastrum genus. *Syncephalastrum timoneanum* PMMF0107 seemed closer to *S. racemosum* DSM 859 and *Syncephalastrum massiliense* PMMF0073 was closer to *S. monosporum* clade. The phylogenetic tree constructed using the four loci was congruent with the MALDI-TOF MS dendrogram and showed the same species clustering.

All strains shared the following macroscopic features: colony texture, time and temperature of growth as previously described [8,36]. Moreover, the mycelium colour of the new isolates was akin to *S. monosporum*. All the strains did not grow ≥40 °C. In contrast to our observations, some authors have described *S. racemosum* and *S. monosporum* as hydrophilic and thermotolerant moulds [12], or have declared that *Syncephalastrum* species were able to grow above 40 °C [6,10].

S. racemosum can be misidentified and confused with some black *Aspergillus* species, such as *Aspergillus niger* [5].The hyphal morphology and the merosporangial sack enclosing sporangiospores are key to differentiating these two fungi, but also to distinguishing between *Syncephalastrum* species. According to Hoffman et al. (2013) [37], *Syncephalastrum* is the only genus in the *Mucorales* which produces merosporangia with the merospores arranged in linear chains. Benjamin RK (1959) [22] also reported that *S. racemosum* produces sporangiospores in deciduous, tubular merosporangial sacks developed across the entire surface of an apical, spherical swelling of the sporangiophore. Indeed, microscopic features are very useful for these fungi classifications. In fact, the two new isolated strains share many *S. racemosum* morphological features, mainly relying on the number of sporangiospores contained in each merosporangial sack. *S. racemosum* merosporangium contains about six or seven sporangiospores, while *S. monosporum* contains only one sporangiola. In all the strains, hyphae are large, aseptate with a ribbon-like aspect as described in Gomes et al. (2011) [10]. Several comprehensive studies [38–40], based on *Mucorales* antifungal susceptibility testing reported significant variation between genera, species and strains within the *zygomycetes* class. The three species of *S. massiliense* PMMF0073, *S. timoneanum* PMMF0107 and *S. racemosum* DSM 859 were uniformly susceptible to Amphotericin B and itraconazole. However, only *S. timoneanum* PMMF0107 and *S. racemosum* DSM 859 were susceptible to posaconazole. The susceptibility displayed by *S. racemosum* against the three antifungal drugs has already been reported by Vitale et al. 2012 [41]. In line with the microscopic analyses, the antifungal susceptibility profiles of the two novel species, *S. timoneanum* PMMF0107 and *S. massiliense* PMMF0073, were relatively closer to *S. racemosum* than to *S. monosporum.*

While molecular methods and phenotypic methods such as MALDI-TOF MS and morphological analysis supply no information about strain properties, the Biolog™ system provides information on the assimilation capacity of fungus carbon sources. Whereas the majority of the substrates were assimilated by all strains, some relevant differences were helpful in discriminating between the two isolates. *S. massiliense* PMMF0073 was the strain that assimilated the least substrates. Among the substrates assimilated by all except *S. massiliense* PMMF0073 are adonitol, α-methyl-D-glucoside, trehalose, turanose, succinic acid mono-methyl ester, and alaninamide. One exception was D-tagatose, which was assimilated by *S. massiliense* PMMF0073, and not by *S. timoneanum* PMMF0107. In contrast, *S. timoneanum* PMMF0107 was the only species that assimilated almost all substrates, except D-tagatose, D-psicose, N-acetyl-D-mannosamine, L-fucose, glucuronamide, and sedoheptulosan. On the basis of these carbon source assimilation profiles, *S. timoneanum* PMMF0107 was close to *S. monosporum* species, and *S. massiliense* PMMF0073 was close to *S. racemosum* DSM 859. Besides, relying on the EDX chemical mapping, the new strains were fairly similar to the *S. monosporum* species. Finally, the morphological features, antifungal susceptibility tests, and the ITS and D1D2 tree highlighted the similarities of both *S. massiliense* and *S. timoneanum* with *S. racemosum*.

Conclusion

The two novel species in the genus *Syncephalastrum*, *S. massiliense* PMMF0073 and *S. timoneanum* PMMF0107 have a similar morphology to *S. racemosum* but each displays distinct phenotypic and genotypic features. The polyphasic approach, combining the results of complementary assays, including the Biolog™ system, MALDI-TOF MS, and EDX, was instrumental in describing and characterising these two new *Syncephalastrum* species.

Authors' contributions: Conceptualisation, JK and SR; Methodology, SR, JK, MM; Formal analysis, JK, MM, FB, SR; Writing original draft, JK; Writing-review and editing, SR, FB, MM. All authors have read and agreed to the final version of the manuscript.

Funding: This research was funded by the Institut Hospitalo-Universitaire (IHU) Méditerranée Infection and by the French Government under the "Investissements d'avenir" (Investments for the Future) program managed by the Agence Nationale de la Recherche (ANR, fr: National Agency for Research), (reference: Méditerranée Infection 10-IAHU-03) and the Région Provence-Alpes-Côte d'Azur, European ERDF funding (European regional development fund) and PRIMMI ((Plateformes de Recherche et d'Innovation Mutualisées Méditerranée Infection).

Availability of data and materials: The *Syncephalastrum massiliense* holotype is available at the IHU MI (No PMMF0073) and IHEM (No 28561) strain collections. The nucleotide sequences are available on GenBank (Accession Numbers: OL699905, ON149883, OM362516 and OM417069). The datasets analysed during the current study are available from the corresponding author on reasonable request. The *Syncephalastrum timoneanum* holotype is available at the IHU MI (No PMMF0107) and IHEM (No 28562) strain collections. The nucleotide sequences are available on GenBank (Accession Numbers: OL699906, ON149884, OM362517 and OM417070).

Acknowledgments: The authors acknowledge the technical support of Anthony Fontanini for electron microscopy analyses. We sincerely thank Takashi Irie, Kyoko Imai, Shigeki Matsubara, Taku Sakazume, Toshihide Agemura and the Hitachi team in Japan for the collaborative study conducted together with IHU Méditerranée Infection, and the installation of TM4000 Plus microscopes at the IHU Méditerranée Infection facility.

Competing interests: The authors declare that they have no competing interests.

List of Abbreviations

DNA	deoxyribonucleic acid
GC	Gentamycin and Chloramphenicol
HIV	Human Immunodeficiency Virus
IHU Méditerranée Infection	Institut Hospitalo-Universitaire Méditerranée Infection
ITS	rRNA Internal Transcribed Spacers
SDA	Sabouraud Dextrose Agar
LSU	large-subunit of the rRNA
MALDI-TOF MS	Matrix-assisted Laser Desorption/ Ionization Time of Flight Mass Spectrometry
MP	Maximum Parsimony
NA	Not available
PCA	Principal Component Analysis
rRNA	ribosomal ribonucleic acid
SSU	small-subunit of the rRNA
TEF-1-α	partial Translation Elongation Factor 1-alpha gene
TUB2	partial β-tubulin gene

References

1. Amatya, R.; Khanal, B,; Rijal, A. *Syncephalastrum* Species Producing Mycetoma-like Lesions. *Indian Journal of Dermatology, Venereology, and Leprology*. **2010,** 3, 76–284. https://doi.org/10.4103/0378-6323.62977
2. Horner, W.E.; Worthan, A.G.; Morey, P.R. Air- and Dustborne Mycoflora in Houses Free of Water Damage and Fungal Growth. *Applied and Environmental Microbiology*. **2004**, 11, 6394–6400. https://doi.org/10.1128/AEM.70.11.6394-6400.2004
3. Ogunlana, E.O. Fungal Air Spora at Ibadan, Nigeria . *Applied Microbiology*. **1975**, 4, 63–458. https://doi.org/10.1128/am.29.4.458-463.1975

4. Rao, C.Y.; Kurukularatne, C.; Garcia-Diaz, J.B.; Kemmerly, S.A.; Reed, D.; Fridkin, S.K.; Morgan, J. Implications of Detecting the Mold Syncephalastrum in Clinical Specimens of New Orleans Residents After Hurricanes Katrina and Rita. *Journal of Occupational & Environmental Medicine*. **2007**, 4, 16–411. https://doi.org/10.1097/JOM.0b013e31803b94f9
5. Ribes, J.A.; Vanover-Sams, C.L.; Baker, D.J. *Zygomycetes* in Human Disease. *Clinical Microbiology Reviews*. **2000**, 2, 236–301. https://doi.org/10.1128/CMR.13.2.236
6. Mangaraj, S.G.S.; Patro, M.K.; Padhi, S. A Rare Case of Subcutaneous Mucormycosis Due to *Syncephalastrum Racemosum*: Case Report and Review of Literature. *Indian Journal of Medical Microbiology*. **2014**, 4, 51–448. https://doi.org/10.4103/0255-0857.142252
7. Mathuram, A.J.; Mohanraj, P.; Mathews, M.S.; Rhino-Orbital-Cerebral Infection by *Syncephalastrum Racemosusm*. *The Journal of the Association of Physicians of India*. **2013**, 5, 40–339.
8. Baby, S.; Ramya, T.G.; Geetha, R.K. Onychomycosis by *Syncephalastrum Racemosum*: Case Report from Kerala, India. *Dermatology Reports*. **2015**, 7, 5527. https://doi.org/10.4081/dr.2017.5527
9. Baradkar, V.P.; Mathur, M.; Panda, M.; Kumar, S. Sino-orbital infection by *Syncephalastrum racemosum* in chronic hepatorenal disease. *J Oral Maxillofac Pathol*. **2008**, 12, 7–45. https://doi.org/10.4103/0973-029X.42199
10. Gomes, M.Z.R.; Lewis, R.E.; Kontoyia, nnis, D.P. Mucormycosis Caused by Unusual Mucormycetes, Non-*Rhizopus*, -*Mucor*, and -*Lichtheimia* Species. *Clinical Microbiology Reviews*. **2011**, 2, 45–411. https://doi.org/10.1128/CMR.00056-10
11. Irshad, M.; Nasir, N.; Hashmi, U.H.; Farooqi, J.; Mahmood, S.F. Invasive Pulmonary Infection by *Syncephalastrum* Species: Two Case Reports and Review of Literature. *IDCases*. **2020**, 21, 00913. https://doi.org/10.1016/j.idcr.2020.e00913
12. Rodríguez-Gutiérrez, G.; Carrillo-Casas, E.M.; Arenas, R.; García-Méndez, J.O.; Toussaint, S.; Moreno-Morales, M.E.; Schcolnik-Cabrera, A.A.; Xicohtencatl-Cortes, J.; Hernández-Castro, R. Mucormycosis in a Non-Hodgkin Lymphoma Patient Caused by *Syncephalastrum Racemosum*: Case Report and Review of Literature. *Mycopathologia*. **2015**, 2, 89–93. https://doi.org/10.1007/s11046-015-9878-1
13. Ramesh, V.; Ramam, M.; Capoor, M.R.; Sugandhan, S.; Dhawan, J.; Khanna, G. Subcutaneous Zygomycosis: Report of 10 Cases from Two Institutions in North India: Subcutaneous Zygomycosis. *Journal of the European Academy of Dermatology and Venereology*. **2010**, 10, 25–1220. https://doi.org/10.1111/j.1468-3083.2010.03606.x
14. Schlebusch, S.; Looke, D.F.M. Intraabdominal Zygomycosis Caused by *Syncephalastrum Racemosum* Infection Successfully Treated with Partial Surgical Debridement and High-Dose Amphotericin B Lipid Complex. *Journal of Clinical Microbiology*. **2005**, 11, 27–5825. https://doi.org/10.1128/JCM.43.11.5825-5827.2005
15. Voigt, K.; Cigelnik, E.; O'donnell, K. Phylogeny and PCR Identification of Clinically Important *Zygomycetes* Based on Nuclear Ribosomal-DNA Sequence Data. *Journal of Clinical Microbiology*. **1999**, 12, 64–3957. https://doi.org/10.1128/JCM.37.12.3957-3964.1999
16. Zaki, S.M.; Elkholy, I.M.; Elkady, N.A.; Abdel-Ghany, K. Mucormycosis in Cairo, Egypt: Review of 10 Reported Cases. *Medical Mycology*. **2013**, 1–8. https://doi.org/10.3109/13693786.2013.809629.
17. Vander, Straten, R.M.; Balkis, M.M.; Ghannoum, A.M. The role of nondermatophyte molds in onychomycosis: diagnosis and treatment. *Dermatologic Therapy*. **2002**, 15, 89–98. https://doi.org/10.1046/j.1529-8019.2002.01522.x
18. Gupta, A.K.; Ryder, J.E.; Baran, R.; Summerbell, R.C. Non Dermatophyte Onychomycosis. *Dermatologic Clinics*. **2003**, 2, 68–257. https://doi.org/10.1016/S0733-8635(02)00086-4
19. Schroter, J.; Kryptogamen-Flora, von Schlesien: Pilze. Breslau: J.U. Kern. **1908**.
20. Urquhart, A.S.; Idnurm, A. *Syncephalastrum Contaminatum*, a New Species in the *Mucorales* from Australia. *Mycoscience*. **2020**, 3, 15–111. https://doi.org/10.1016/j.myc.2020.02.003
21. Benjamin, R.K. The merosporangiferous *Mucorales*. *Aliso*. **1959**, 4, 321–433.
22. O'Donnell K, Lutzoni F.M.; Ward, T.J.; Benny, G.L. Evolutionary relationships among mucoralean fungi (*Zygomycota*): evidence for family polyphyly on a large scale. *Mycologia*. **2001**, 93, 286–296.
23. Schwarz, P.; Bretagne, S.; Gantier, J.C.; Garcia-Hermoso, D.; Lortholary, O.; Dromer, F.; Dannaoui, E. Molecular identification of *zygomycetes* from culture and experimentally infected tissue. *J. Clin. Microbiol*. **2006**, 44, 340–349.
24. Cassagne, C.; Normand, A.C.; L'Ollivier, C.; Ranque, S.; Piarroux, R. Performance of MALDI-TOF MS Platforms for Fungal Identification. *Mycoses*. **2016**, 59, 90–678. https://doi.org/10.1111/myc.12506

25. Normand, A.C.; Cassagne, C.; Gautier, M.; Becker, P.; Ranque, S.; Hendrickx, M.; Piarroux, R. Decision criteria for MALDI-TOF MS-based identification of filamentous fungi using commercial and in-house reference databases. *BMC Microbiol.* **2017**, 1, 25. doi: 10.1186/s12866-017-0937-2.
26. White, T.J.; Bruns, T.; Lee, S.; Taylor, J. Amplification and direct sequencing of fungal ribosomal RNA genes for phylogenetics. *In PCR Protocols.* **1990**, 18, 22–315.
27. Glass, N.L.; Donaldson, G.C. Development of Primer Sets Designed for Use with the PCR to Amplify Conserved Genes from Filamentous Ascomycetes. *Applied and Environmental Microbiology*. **1995**, 61, 30–1323. https://doi.org/10.1128/aem.61.4.1323-1330.1995
28. Carbone, I.; Kohn, L.M. A Method for Designing Primer Sets for Speciation Studies in Filamentous Ascomycetes. *Mycologia*, **1999**, 91, 553–556.
29. De Hoog, G.S.; Guarro, J.; Gené, J.; Figueras, M.J. Atlas of Clinical Fungi, 2nd ed.; Universitat Rovira i Virgili Reus: Tarragona, Spain; Centraalbureau voor Schimmelcultures: Utrecht, The Netherlands, **2000**.
30. Tamura, K.; Stecher, G.; Kumar, S. MEGA11: Molecular Evolutionary Genetics Analysis Version 11. Édité par Fabia Ursula Battistuzzi. *Molecular Biology and Evolution*. **2021**, 7, 27–3022. https://doi.org/10.1093/molbev/msab120.
31. Kabtani, J.; Militello, M.; Ranque, S. *Coniochaeta massiliensis* sp. nov. Isolated from a Clinical Sample. *J. Fungi*. **2022**, 8, 999. https://doi.org/10.3390/jof8100999
32. Bochner, B.R. Phenotype MicroArrays for High-Throughput Phenotypic Testing and Assay of Gene Function. *Genome Research*. **2001**, 11, 55–1246. https://doi.org/10.1101/gr.186501
33. Pinzari, F.; Nadir, Abu-Samra, A.C.; Canfora, L.; Maggi, O.; Persiani, A. Phenotype MicroArray™ System in the Study of Fungal Functional Diversity and Catabolic Versatility. *Research in Microbiology*. **2016**, 9, 22–710. https://doi.org/10.1016/j.resmic.2016.05.008
34. Kondori, N.; Svensson, E.; Mattsby-Baltzer, I. In Vitro Susceptibility of Filamentous Fungi to Itraconazole, Voriconazole and Posaconazole by Clinical and Laboratory Standards Institute Reference Method and E-Test: In Vitro Susceptibility of Filamentous Fungi. *Mycoses*. **2011**, 5, 22–318. https://doi.org/10.1111/j.1439-0507.2010.01913
35. Yang, M.; Lee, J.H.; Kim, Y.K.; Ki, C.S.; Huh, H.J.; Lee, N.Y. Identification of Mucorales From Clinical Specimens: A 4-Year Experience in a Single Institution. *Annals of Laboratory Medicine*. **2016**, 1, 60–63. https://doi.org/10.3343/alm.2016.36.1.60
36. Hoffmann, K.; Pawłowska, J.; Walther, G.; Wrzosek, M.; de Hoog, G.S.; Benny, G.L.; Kirk, P.M.; Voigt, K. The Family Structure of the *Mucorales*: A Synoptic Revision Based on Comprehensive Multigene-Genealogies. *Persoonia - Molecular Phylogeny and Evolution of Fungi*. **2013**, 30, 57–76. https://doi.org/10.3767/003158513X666259.
37. Dannaoui, E. ; Meletiadis, J.; Mouton, J.W. ; Meis, J.F. ; Verweij, P.E. In vitro susceptibilities of *zygomycetes* to conventional and new antifungals. *J. Antimicrob. Chemother*. **2003**, 51, 45–52.
38. Torres-Narbona, M.; Guinea, J.; Martinez-Alarcon, J.; Pelaez, T.; Bouza, E. In vitro activities of amphotericin B, caspofungin, itraconazole, posaconazole, and voriconazole against 45 clinical isolates of *zygomycetes*: comparison of CLSI M38-A, Sensititre YeastOne, and the Etest. *Antimicrob. Agents Chemother*. **2007**, 51, 1126 –1129.
39. Almyroudis, N.G.; Sutton, D.A.; Fothergill, A.W.; Rinaldi, M.G.; Kusne, S. In vitro susceptibilities of 217 clinical isolates of *zygomycetes* to conventional and new antifungal agents. *Antimicrob. Agents Chemother.* **2007**, 51, 2587–2590.
40. Vitale, R.G.; de Hoog, G.S.; Schwarz, P.; Dannaoui, E.; Deng, S.; Machouart, M.; Voigt, K. Antifungal Susceptibility and Phylogeny of Opportunistic Members of the Order *Mucorales*. *Journal of Clinical Microbiology*. **2012**, 50, 66–75. https://doi.org/10.1128/JCM.06133-11.